공학석사 학위논문

Anti-Allergic Effect of Polyphenol Mixture in Atopic Dermatitis using Double Emulsion-Mediated Delivery

아토피 모델에서의 이중 에멀젼 매개 전달을 이용한 폴리페놀 혼합물의 항알레르기 효과

2023 년 8 월

서울대학교 대학원

공과대학 협동과정 바이오엔지니어링전공

최 수 빈

Anti-Allergic Effect of Polyphenol Mixture in Atopic Dermatitis using Double Emulsion-Mediated Delivery

지도 교수 황 석 연

이 논문을 공학석사 학위논문으로 제출함
2023 년 8 월

서울대학교 대학원
공과대학 협동과정 바이오엔지니어링 전공

최 수 빈

최수빈의 공학석사 학위논문을 인준함
2023 년 8 월

위 원 장 _____ (인)

부위원장 _____ (인)

위 원 _____ (인)

Abstract

Polyphenol has been studied for its various biological activities, including anti-inflammation, anti-oxidant, and anti-viral. Herein, we conducted a screening of the polyphenol mixture (PM) to identify the optimal composition and ratio of polyphenols. These PMs are designed for application to atopic dermatitis (AD) and are expected to have a synergistic efficiency than single polyphenols. However, there are still challenges to developing the method for delivering with stabilized formulation, due to the susceptibility to oxidation, low solubility, and low miscibility of polyphenol. Therefore, we applied the water-in-oil-in-water double emulsion (W/O/W) system to deliver the PM. Through the *in vitro* anti-degranulation assay results, we screened the particular molar ratio of PM (Q:P:E=5:1:1) and confirmed the therapeutic window. In addition, we verified the advantage of the W/O/W over oil-in-water single emulsion (O/W) as a proper nanocarrier for PM. In the *in vivo* 1-chloro-2,4-dinitrobenzene (DNCB)-induced mice AD model, PM-encapsulated W/O/W (PM_W/O/W) represented the most effectiveness in AD alleviation compared to single polyphenols and PM by clinical, histological, and immunological analysis. Eventually, this research suggests a novel AD therapeutic system by encapsulating the optimal ratio of polyphenol mixture in double emulsion and shows the possibility of the appliance to other allergic diseases.

Keyword : Polyphenol, Double Emulsion, Nanocarrier, Transdermal Drug Delivery, Atopic Dermatitis, Allergy
Student Number : 2021-20946

Table of Contents

Chapter 1. Introduction

1.1. Atopic Dermatitis (AD)

Skin is the outermost tissue which protects the body against mechanical, chemical stress, temperature, UV, and microbes. Therefore, abnormal skin barrier induced by genetic and environmental factors can destroy the overall skin physiology which can cause various diseases. Atopic dermatitis (AD) is one of the worldwide inflammatory skin diseases which is non-contagious and shows symptoms including dryness, itching, and redness [1-3]. Especially, the enhanced Th2 polarization is the key pathway of developing AD though the entire mechanism of developing AD has not been fully identified [4]. Activated Th2 cell increases the expression of pro-inflammatory cytokines such as IL-4, IL-5, and IL-13, resulting in an excessive immune response and production of Immunoglobulin E (IgE) from B cells. The expressed IgE mediated the allergic reaction by degranulating the immune cells, like mast cells and basophils.

Traditional clinics for AD patients involve the use of creams to maintain skin moisture and prescription immunosuppressants, such as pimecrolimus and tacrolimus, which are topical calcineurin inhibitors (TCIs) [5]. However, due to potential side effects like an increased risk of cancer, fever, agitation, and inflammatory shock, these conventional drugs should be used at low concentrations and for short periods, especially in

severe cases of AD [6–9]. Moreover, there has been an increase in the number of AD patients, with a particularly high prevalence in infants and adolescents [10, 11]. For these reasons, the demand for developing novel milder drugs or therapy for AD, such as phytochemical or natural compound–based drugs, has been studied for low inflammatory side effects by directly controlling allergic response rather than systemic immune response [12, 13].

1.2. Polyphenol Mixture (PM)

1.2.1. Polyphenol

In this study, we used naturally occurring phytochemicals, called polyphenols, which have aromatic rings with several hydroxyl groups. Currently, more than 8,000 types of polyphenols have been reported. Polyphenol has several potential health benefits including anti–oxidant, anti–inflammatory, blood cholesterol level mitigation effect, and anti–allergic effects [14, 15]. Therefore, these biological effects make polyphenols to be used as healthcare foods or therapeutics for various diseases; e.g. cancer, obesity, diabetes, bone, and cardiovascular diseases [14, 16–19]. Especially, quercetin (Q), phloretin (P), and ellagic acid (E), which are frequently used in the healthcare and therapeutics industries, were used in this study. The Q upregulates the Th1–mediated immune response and simultaneously downregulates the

Th2-mediated immune response in AD [20-22]. Considering AD patients have over-activated Th2-mediated immune responses, we can deal with the Q as a therapeutic for AD. In addition, the pro-inflammatory cytokines, such as interleukin (IL)-4, IL-6, IL-17A, interferon γ (IFN-γ), and thymic stromal lymphopoietin (TSLP) can be alleviated by the P. The previous study showed the AD mitigation effect of P through the inhibition of mitogen-activated protein kinase (MAPK) and nuclear factor kappa-light-chain-enhancer of activated B cells (NF-κB) signaling pathway [23, 24]. Also, the E regulates MAPK and signal transducer and activator of the transcription (STAT) signaling pathway. In the DfE-induced AD mouse model, E reduces the level of IL-6 expression and immunoglobulin E (IgE) [25].

However, studies of AD therapy so far only elucidated the therapeutic effect of single polyphenols alone or polyphenol extract which consist of several polyphenols whose exact proportions are unknown. Therefore, to maximize the biological effect and consistently prescribe the exact therapeutic solution to patients, we screened a specific ratio of polyphenol mixture (PM) which is the most suitable as an AD treatment by introducing the keyword, called combination drug therapy.

1.2.2. Combination Drug Therapy

Combination drug therapy is a therapeutic method that prescribes multiple active substances that target the same disease with the same or

different pathways at a time. This method shows a biological synergetic effect than the same amount of each drug alone and reduces side effects and considerable factors. Thus, combination drug therapy has recently increased interest in clinical medicine [26-29]. Moreover, combination drug therapy has great advantages in that they minimize the time and cost of developing new clinics with better effects. According to prior studies, a suitable carrier that delivers the drug sustainably and uniformly is required to deliver the desired drugs at an accurate drug combination ratio with a single dose [26].

To increase skin penetration efficiency and stabilize the polyphenols (Q, P, E), which have low solubility and miscibility and are used as a drug in this study, we attempted to use double emulsion as transdermal delivery carriers.

1.3. Double Emulsion

Microemulsions are thermodynamically stable, isotropic mixtures of oil, water, and surfactant, frequently in combination with a co-surfactant [30-33]. It was applied as a drug delivery carrier in various fields, such as therapeutics, food, and healthcare products. Most of the microemulsion is formed by a definite amphiphilic surfactant boundary between the oil phase and the water phase. Additionally, microemulsion represents several microstructures, including oil-in-water (O/W) and water-in-oil (W/O)

[33]. The volume of oil is much higher than water, so the water phase is isolated by the surfactant to form particles in the oil phase is called W/O microemulsion. And the opposite case of oil and water phase volume is called O/W microemulsion. In other words, the smaller volume phase forms the droplets and another phase was comprised overall solvent. Furthermore, multiple emulsions have various advantages over single emulsions (e.g. W/O, O/W microemulsion). Double emulsion, which is classified as water-in-oil-in-water (W/O/W) and oil-in-water-in-oil (O/W/O), was the most common type of multiple emulsions [34, 35]. This nanocarrier could encapsulate the hydrophilic components in the water phase, hydrophobic components in the oil phase, and amphiphilic components in the amphiphilic interphase between water and oil phase [36]. To fabricate the double emulsion which has the appropriate size for delivery, two steps are commonly performed. Primarily, the single emulsion (W/O or O/W microemulsion) is formed. And then, an additional water or oil phase was fabricated by applying extra force, such as ultrasonication and microfluidics [37, 38].

1.4. Research aims

In this study, we have suggested an optimal ratio of PM which showed a synergetic effect and suppressed the side effects of single polyphenols. The relative release level of β-hexosaminidase was used to compare the anti-allergic effect on *in vitro* model, followed by choosing the specific molar ratio of PM as well as its therapeutic window. To overcome the limitations of polyphenols such as the susceptibility to oxidation, low solubility, and low miscibility, we introduced a water-in-oil-in-water double emulsion (W/O/W) as a drug delivery nanocarriers. Eventually, we estimated the AD alleviation efficacy of PM-encapsulated water-in-water double emulsion (PM_W/O/W) by comparing to other polyphenol groups in the DNCB-induced AD mice model by clinical, histological, and immunological analysis.

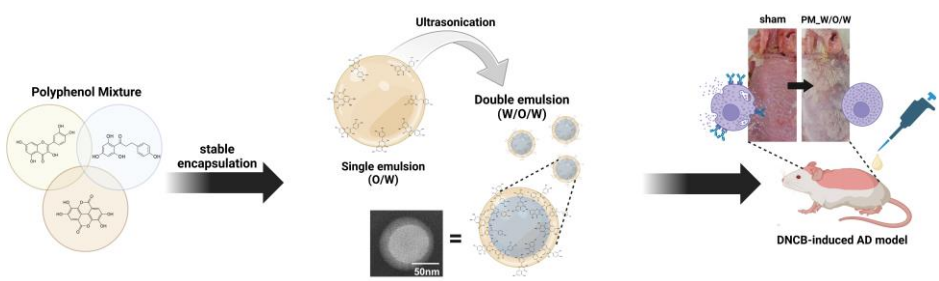

Scheme 1. Schematic illustration of fabrication of PM_W/O/W and its transdermal delivery on *in vivo* atopic dermatitis model.

Chapter 2. Materials and Methods

2.1. Preparation of polyphenol mixture and drug delivery carrier

Quercetin (Q), phloretin (P), and ellagic acid (E) were purchased from UAT Corporation (Republic of Korea) as food grades. In this study, a polyphenol mixture (PM) was designed with an specific composition and ratio of polyphenols (Q:P:E = 5:1:1). To encapsulate PM in water-in-oil-in-water double emulsion (W/O/W), olive oil (Sigma) was used for oil phase to dissolve polyphenols and distilled water was used for water phase of the emulsion. Transcutol® P (diethylene glycol monoethyl ether) and Labrasol® (caprylocaproyl polyoxyl-8 glycerides) were used as surfactants to increase the stability of the emulsion and were provided by Gattefossé (France). To formulate oil-in-water single emulsion (O/W), surfactants (Transcutol® P, 1.6 v/v%; Labrasol®, 0.4 v/v%) and distilled water (DW, 96.5 v/v%) were added to the oil phase (olive oil, 1.5 v/v%). After O/W formulation, we performed ultrasonication (5 min, 30% amplitude, 5 s pulse/5 s rest) to fabricate W/O/W. Then, we removed residuals by dialysis with 3.5K MWCO membrane (SnakeSkin^{TM} Dialysis Tubing; 35 mm, Sigma) for 2h.

2.2. Cell culture

HaCaT cell (human keratinocyte cell line) was cultured in Dulbecco Modified Eagle Medium (DMEM, Hyclone) with 15% fetal bovine serum (FBS, Corning), 1% Penicillin/Streptomycin (PS, 10,000 U/mL, Gibco^{TM}). RBL-2H3 (rat basophil cell line) was purchased from ATCC (United States). The culture media of RBL-2H3 was used by adding 15% FBS and 1% PS to Modified Eagle Medium (MEM, Gibco^{TM}). Each cell culture plate was incubated at 37 ℃ under 5 v/v% CO_2 with humidity.

2.3. *in vitro* biocompatibility of polyphenols

Live/Dead assay was used to assess the cytotoxicity of polyphenols. HaCaT cells were seeded in 24-well plates at 20,000 cells per well, and each group was triplicated (n=3). The sample was prepared at molar concentrations of 5, 10, 25, and 50 μM for each single polyphenol (Q, P, E) and 50 μM for PM. Each sample was treated for 24h, then stained with calcein AM (calcein acetoxymethyl ester) and ethidium homodimer (ethD-1). To quantify the cell viability, the number of live cells was divided by the number of total cells based on the image of the EVOS XL Core Cell Imaging System through the ImageJ software.

Counting Kit-8 (CCK-8, Dojindo Laboratories) assay was used to confirm the effect of cell proliferation. The sample was also prepared at molar concentrations of 5, 10, 25, and 50 μM for each single polyphenol

(Q, P, E). HaCaT cells were seeded in a 96-well plate at 2,500 cells per well, and each group was triplicated (n=3). After 24h, cells were incubated with 10 μL CCK-8 solution for 3 h and quantified by UV/VIS spectroscopy (TECAN Infinite M200 Pro, Tecan, Swiss) at 450nm.

2.4. *in vitro* anti-allergic effect of PM

RBL-2H3 cells were seeded in 24-well plates at 100,000 cells per well and each group was triplicated (n=3). After 24 h stabilization at 37 ℃ incubator, monoclonal anti-dinitrophenyl antibody (produced in mouse, IgE, Sigma) was treated for 24h at 37 ℃. Then each sample was treated for 1h. To activate the RBL-2H3 cells, 1 μg/mL DNP-Albumin Conjugate (DNP-HSA, Sigma), which is dissolved in extracellular buffer with 0.1 w/v% Bovine Serum Albumin (BSA, Albumin, Ultrapure, GeneDEPOT) was treated for 3h at 37 ℃. After sensitization, cell supernatant and cell lysis were reacted with 1 mM *p*-nitrophenyl N-acetyl glucosaminide dissolved in 0.05 M citrate buffer (pH 4.5) for 1 h at 37 ℃. Then, by adding 0.1 M sodium carbonate (Na_2CO_3) (pH 10), the reaction was finished. Consequently, the reactant was transferred to 96-well and was measured absorbance at 405nm using UV/VIS spectroscopy. The relative amount of degranulation rate of basophil can be quantified through the relative absorbance value.

2.5. Characterization of Double emulsion

The appearance and color of emulsions was observed on day 1, 3, 5, and 7. Formation of the W/O/W and O/W were imaged by Field Emission TEM (200kV; JEM-F200, JEOL Ltd, Japan). The samples were stained with 0.2% phosphotungstic acid (Sigma) to be a negative charge. The negatively stained sample was loaded on the TEM grid (CF200-CU, EMS, United States). The biphasic microstructure and the encapsulated drug property in W/O/W were confirmed by Confocal Laser Scanning Microscope (CLSM) (LSM980, Carl Zeiss, Germany).

Total phenolic content (TPC) assay was performed to identify the encapsulated concentration of the PM in W/O/W and O/W. 20 μL of 1N Folin & Ciocalteu's phenol reagent (Sigma) was added to 80 μL of samples in a 96-well plate for 5 min at room temperature (RT). Consequently, 100 μL of 2% Na_2CO_3 was treated for 1 h without light. Total phenol contents were estimated by measuring the absorbance at 750 nm with a spectrophotometer (Varioskan LUX Plate Reader, ThermoFisher Scientific, Finland).

Size, zeta-potential, and stability of O/W, PM-encapsulated O/W (PM_O/W), W/O/W, and PM-encapsulated W/O/W (PM_W/O/W) were observed by dynamic light scattering device (DLS; Zetasizer Nano ZS, Malvern, United Kingdom).

2.6. *in vivo* atopic dermatitis-induced model

BALC/c mice (6 weeks old, male; n=3 per group) were purchased from Orient-Bio (Republic of Korea). All animal experiments were approved by the Institutional Animal Care and Use Committee at Seoul National University (Registration No. SNU-210910-2-2). The laboratory conditions were set up temperature of 22±2 ℃, humidity 50±5%, and light/dark cycle: 12h. 1-Chloro-2,4-dinitrobenzene (DNCB, Sigma) was widely used to induce atopic dermatitis *in vivo* mouse models [39-41]. A day after shaving 4 cm x 1 cm region of dorsal skin from neck to pelvis, 2 w/v% DNCB (dissolved in acetone:olive oil = 3:1) was treated to induce the AD for 3 days of the first week. Then, 200 μL of each sample was treated three times a week for 15 days. During the experiment, to prevent the natural healing of mouse skin and maintain AD sensitization, 0.5 w/v% DNCB was also evenly treated with sample treatment.

The experimental group was divided into seven: (1) negative control group, (2) sham group (DNCB-induced AD), (3) Q group (DNCB-induced AD, 50 μM of Q), (4) P group (DNCB-induced AD, 50 μM of P), (5) E group (DNCB-induced AD, 50 μM of E), (6) PM group (DNCB-induced AD, 50 μM of PM), (7) PM_W/O/W group (DNCB-induced AD, PM-encapsulated W/O/W). To collect the dorsal skin, ears, and serum, mice were euthanized by excess CO_2 inhalation.

To visualize the double emulsions, Nile red was used as the dye due to the similar molar weight and hydrophobicity with polyphenols. IVIS (IVIS Spectrum In Vivo Imaging System, PerkinElmer, United States)

image after 1 h and 24 h sample treatment was obtained to confirm the retention time of double emulsions.

The irritation analysis was performed to evaluate the *in vivo* toxicity of PM and PM_W/O/W based on the erythema index (E). 200 μL PM and PM_W/O/W were treated on shaved dorsal skin. The dermal irritation was estimated based on the L*, a*, and b* values before the treatment, 1 h and 24 h after the sample treatment using a spectrophotometer (CR-400, Konica Minolta Inc., Tokyo, Japan). The intensity of each red (R), blue (B), and green (G) color was calculated by L*, a*, and b* values. The Erythema index (E) was calculated with the following the equation:

$$E = 100 \times \log(\frac{R}{G})$$

2.7. Clinical observation for AD symptoms

Dermatitis score and relative ear thickness assay were conducted to confirm the severity of AD in mice. The skin observations were based on the images and videos taken with the camera in every experiment. The dermatitis score was calculated by Eczema Area and Severity Index (EASI) scoring system. EASI system sums the score with four symptoms; erythema/hemorrhage, scarring/dryness, edema, and excoriation/erosion. Each symptom was evaluated based on 0 (none), 1 (mild), 2 (moderate), and 3 (severe). On days 3, 5, 10, and 15, the ear thickness was measured using a digital clipper micrometer; SD500-150PRO, Seung-Jin, Republic

of Korea). To reduce the error, the ear thickness was measured three times per mouse and was normalized as a relative percentage based on the value of the first measured negative control group.

2.8. Histological analysis of alleviation of AD

1cm x 1 cm mice dorsal skin and ears were fixed with 4 % PFA for 48 h. Consequently, each tissue was paraffin-embedded and sectioned as 10 μm thick on slide glass. Hematoxylin and eosin (H&E) staining was performed to measure epidermal, dermal, and ear thickness. Hematoxylin was purchased from Vector Laboratory and Eosin Y was purchased from Sigma. To count the number of infiltrated mast cells, toluidine blue staining was performed. Toluidine blue was purchased from Sigma. Each stained slide sample was observed using a microscope (Nikon Corporation, Ti), and the data were quantified using Image J Software.

2.9. Measurement of Serum IgE

Serum was harvested using a serum-separating tube with separating gel (BD, 365967) through cardiac puncture. Serum IgE level was measured by mouse Immunoglobulin E, IgE ELISA kit (CSB-E07983m; Cusabio, China).

2.10. Statistical analysis

All the experiments were performed at least triplicated. Data are presented as the mean±standard deviation (SD), and p-values were calculated using one-way ANOVA, and two-way ANOVA (ns, not significant; *$p < 0.05$; **$p < 0.01$; ***$p < 0.001$; ****$p < 0.0001$).

Chapter 3. Results and Discussion

3.1. *in vitro* biocompatibility of polyphenols

To examine the biocompatibility of polyphenols used (Q, P, E) in this study, we confirmed the cellular response by using Live/Dead assay and CCK-8 assay with HaCaT cells. As shown in **Figure 1**, the cell viability of each single polyphenol group and PM group showed at least 98 %. Additionally, the cell proliferation of Q (**Figure 2A**), P (**Figure 2B**), and E (**Figure 2C**) was quantified with CCK-8 assay. When compared to the control group that did not treated Q and P, the cell proliferation rate of both the Q and P groups increased up to 50 μM; especially, cell proliferation rate increased in a concentration-dependent manner up to 25 μM. The cell proliferation rate of E increased below 10 μM, while cell proliferation rate showed decrease over 25 μM of E. These results revealed the low bioavailability and therapeutic windows of single polyphenols *in vitro*.

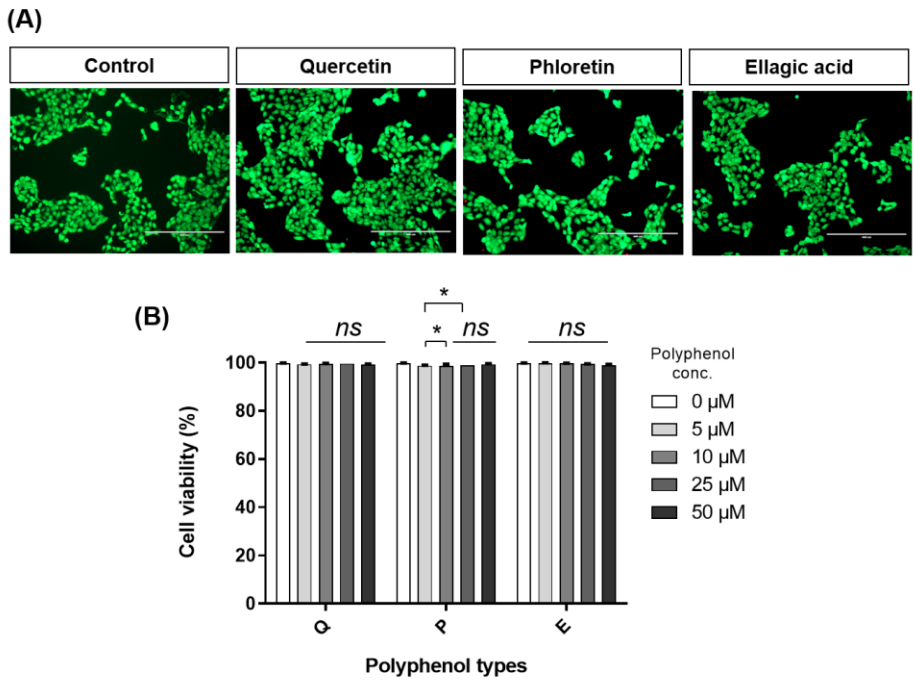

Figure 1. *in vitro* biocompatibility of single polyphenols. Cell viability was estimated by using Live/Dead assay (scale bar = 400 μm). (A) is the image of the 50 μM single polyphenols (quercetin : Q, phloretin : P, and ellagic acid : E) treated group and the control group. (B) By calculating the live cell ratio, cell viability was quantified. (Data are presented as the mean±SD, n=3, and p-values were calculated using two-way ANOVA. ns, not significant; $*p < 0.05$)

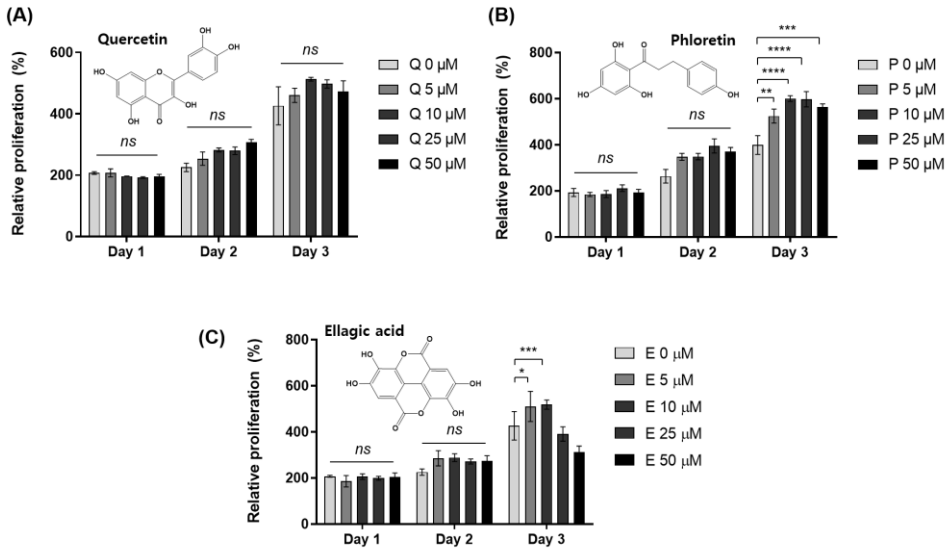

Figure 2. *in vitro* effect on cell proliferation was confirmed by using CCK-8 assay with various concentrations (0, 5, 10, 25, and 50 μM) of (A) Q, (B) P, and (C) E. (Data are presented as the mean±SD, n=3, and p-values were calculated using two-way ANOVA. ns, not significant; $*p < 0.05$; $**p < 0.01$; $***p < 0.001$; $****p < 0.0001$)

3.2. *in vitro* anti-allergic effect of polyphenols

The key factor of atopic dermatitis (AD) is the degranulation of immune cells such as mast cells and basophils. These granules contained various substances including histamine and β-hexosaminidase. We could estimate the severity of allergic response by quantifying the relative amount of released β-hexosaminidase with the IgE-sensitized RBL-2H3 cells which were treated with each single polyphenol at various concentrations (0-50 μM).

Compared to the IgE-only treated positive group, single polyphenols displayed the repressive effect of β-hexosaminidase release at different concentrations. Q showed the lowest β-hexosaminidase release at 25 μM with 78±4.4%, P showed the lowest β-hexosaminidase release at 5 μM with 93.8±4.2%, and E showed the lowest β-hexosaminidase release at 5 μM with 81.7±4.3% **(Figure 3)**. These results showed that Q suppressed degranulation best at 25 μM, P at 5 μM, and E at 5 μM.

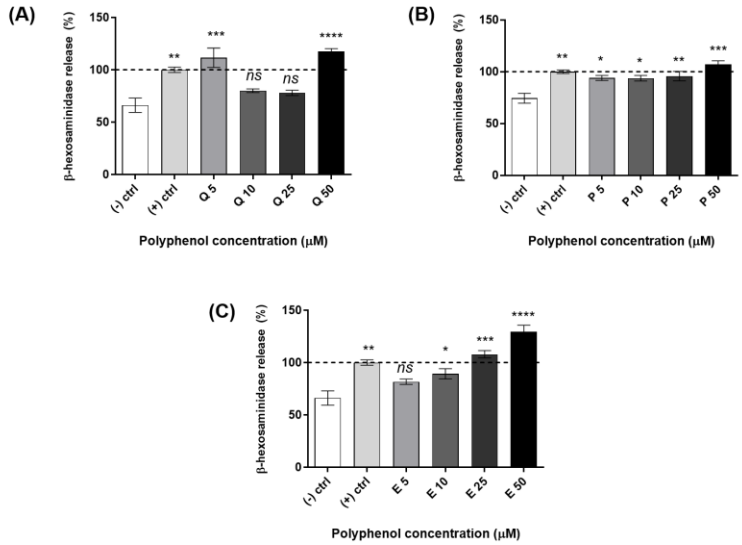

Figure 3. *in vitro* anti-allergic effect of each single polyphenol was confirmed by using β-hexosaminidase assay in RBL-2H3 cell. Each polyphenol was treated with 0, 5, 10, 25, and 50 μM. (Data are presented as the mean$\pm$SD, n=3, and p-values were calculated using one-way ANOVA. ns, not significant; $*p < 0.05$; $**p < 0.01$; $***p < 0.001$; $****p < 0.0001$)

3.3. Screening the specific ratio of PM

Previous studies have demonstrated the various biological efficacy of polyphenols, but few studies have been used with accurate composition and proportions of polyphenols [17, 42, 43]. To overcome the limitations and induce the synergetic effect of polyphenols, we introduced the concept of combinational drug therapy to screen a particular ratio of PM.

There are some recipes of combinational drug therapy that combines two or more drugs with similar structures, functions, and biological properties concerning the most effective therapeutic concentration [44, 45]. Referring to the biocompatibility and the most effective concentration to suppress the allergic response of single polyphenols **(Figure 3A)**, we selected some ratios of PM. As shown in **Figure 4A**, PM with the ratio of Q:P:E=5:1:1 displayed the lowest β-hexosaminidase release level with 85.3±17.3%. The relative level of β-hexosaminidase release at 5:2:1 showed 210±10.2%; 5:1:2 showed 97.9±15.7%; 1:1:1 showed 94.8±12.4%; 2:1:2 showed 121±20.3%; and 2:1:1 showed 182±16.4%. Additionally, two polyphenol combinations was also investigated the anti-allergic effect by β-hexosaminidase release. As shown in **Figure S1**, when the percent of β-hexosaminidase release was 100% in positive group, the Q:P:E = 5:1:1 showed 83.1±6.1%, the Q:P = 5:1 showed 83.66±4.3%, the P:E = 1:1 showed 101±6.1%, and the Q:E = 5:1 showed 88.4±4.8% of β-hexosaminidase release. Considering these results, we selected the PM ratio as Q:P:E=5:1:1, and then PM all refers to a polyphenol mixture with this molar ratio.

In addition, the therapeutic window of PM with Q:P:E = 5:1:1 was confirmed at various concentrations (0−150 μM). It was verified that PM successfully decreased the release of β−hexosaminidase under 100 μM; however, the release of β−hexosaminidase was upsurged over 110 μM (**Figure 4B**). As a result, the PM could increase the bioavailability of polyphenols by expanding the therapeutic window compared to single polyphenols.

In addition, we demonstrated that the addition of another polyphenol (ex. tannic acid, T) to PM hindered the anti−allergic effect of PM. We estimated the biocompatibility of T by using Live/Dead assay and CCK−8 assay **(Figure S2)**. The T has an anti−allergic effect between 5 and 25 μM by quantifying the β−hexosaminidase release **(Figure S3A)**. As shown in **Figure S3B**, when the total polyphenol concentration was 10 μM, PM (Q:P:E=5:1:1) showed the lowest value of β−hexosaminidase release with 56.4±2.8% compared to Q:P:E:T=5:1:1:1 with 77.4±10.4%, 5:1:1:2 with 93.7±17.3%, and 5:1:1:5 with 105±3.1% of β−hexosaminidase release. Additionally, when the total polyphenol concentration was 25 μM, the lowest value of β−hexosaminidase release with 60.4±3.4% was also showed in PM; while Q:P:E:T = 5:1:1:1 showed 97.3±8.8%; Q:P:E:T = 5:1:1:2 showed 106±8.5%; Q:P:E:T = 5:1:1:5 showed 97.4±5.4% of β−hexosaminidase release.

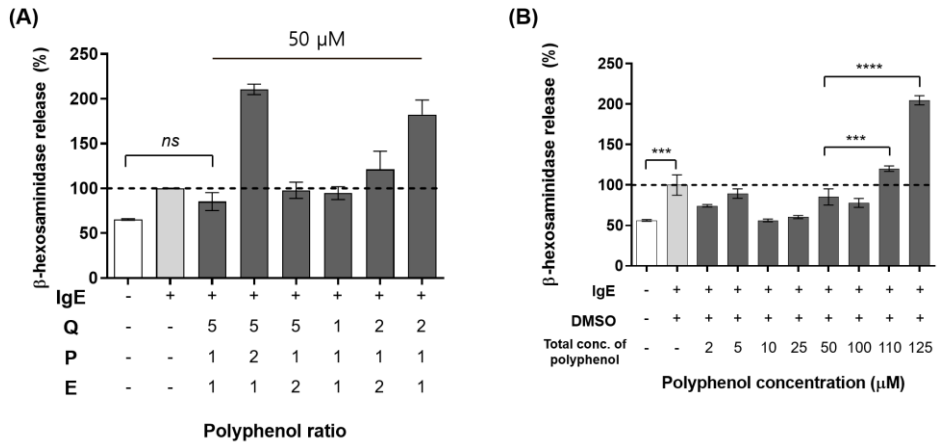

Figure 4. Screening the specific molar ratio of PM. (A) To investigate the optimal molar ratio of PM, the β-hexosaminidase release was estimated with various ratios of PM-treated RBL-2H3 cells. All ratio of PM groups has 50 μM of total polyphenol concentration. (B) The therapeutic window of the optimal PM with Q:P:E=5:1:1 was confirmed by using β-hexosaminidase assay in various concentrations. (Data are presented as the mean±SD, n=3, and p-values were calculated using one-way ANOVA. ns, not significant; ***$p < 0.001$; ****$p < 0.0001$)

3.4. Preparation of PM and drug delivery carrier

To enhance the biocompatibility of polyphenols and transdermally deliver PM simultaneously, the double emulsion (W/O/W) system was applied. We fabricated a W/O/W to stabilize and used it as the transdermal delivery carrier (**Figure 5A**).

By quantifying the total phenyl contents in emulsions, we measured the encapsulation efficiency of PM when the initial total PM concentration increased from 50 to 500 μM. The encapsulation efficiency of PM in W/O/W was significantly increased from 12.1±7 μM to 54±6.6 μM compared to O/W which increase from 6.7±1.3 μM to 11.6±1.3 μM (**Figure 5B**). PM_W/O/W has 418% higher encapsulation of PM than PM_O/W at 500 μM of initial PM concentration. This result showed that the W/O/W more efficiently stabilized the polyphenols and enhanced the encapsulating efficiency than O/W. Thus, we used the PM at 500 μM as the initial loading concentration to fabricate the PM_W/O/W in this study.

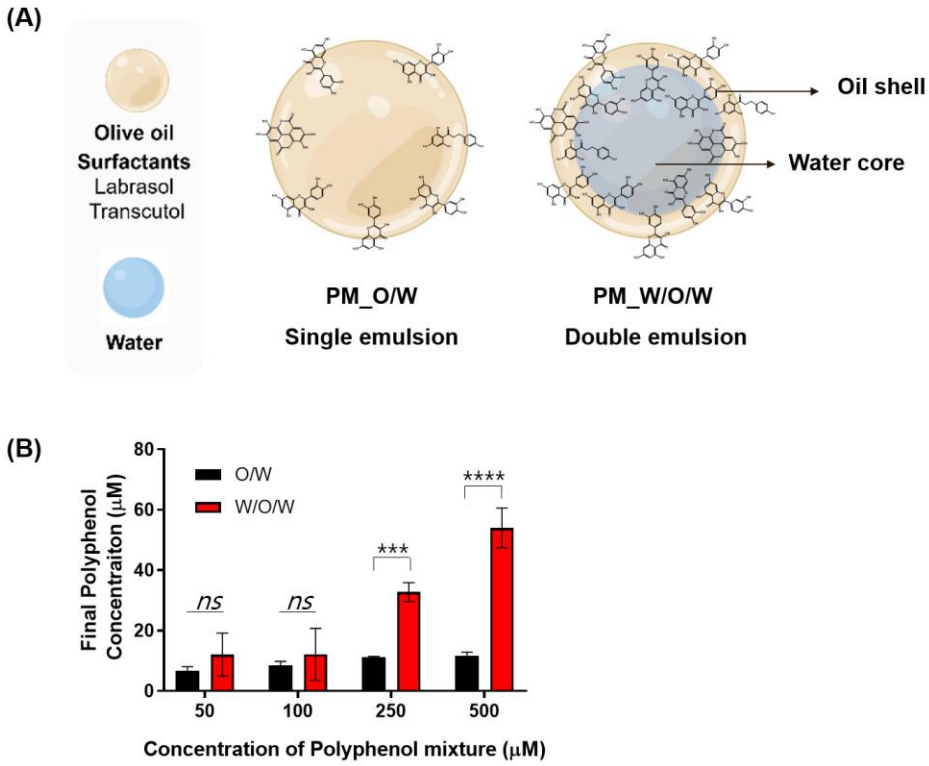

Figure 5. (A) Schematic illustrations of PM-encapsulated oil-in-water single emulsion (PM_O/W) and PM-encapsulated water-in-oil-in-water double emulsion (PM_W/O/W). The illustration was created using Biorender. (B) The encapsulation efficiency of PM based on the initial PM concentration was measured by total phenyl content (TPC) assay. (Data are presented as the mean±SD, n=3, and p-values were calculated using two-way ANOVA. ns, not significant ***$p < 0.001$; ****$p < 0.0001$)

To estimate the fabrication of double emulsions (W/O/W and PM_W/O/W) and single emulsions (O/W and PM_O/W), the appearance and color were observed on day 1, 3, 5, and 7 at RT and 37 ℃. As seen in **Figure S4**, concerning the aggregates of PM_O/W, we demonstrated that the PM is unstably encapsulated in the O/W compared to the W/O/W. Furthermore, the PM entrapped in W/O/W has consistent properties even at RT and 37 ℃ over time. In addition, particle size, surface charge, and stability of emulsions were measured by DLS analysis. The particle diameter of O/W was 673±62.4 nm, and the particle diameter of W/O/W was 197±48.5 nm. PM_O/W showed a particle diameter of 597±10.4 nm and PM_W/O/W showed a particle diameter of 108±1.9 nm (**Figure 6A**). As a result, PM-encapsulated emulsions (PM_O/W and PM_W/O/W) respectively displayed a smaller size than empty emulsions (O/W and W/O/W). The zeta potential of the O/W showed −34.5±0.9 mV and PM_O/W showed −40.3±1.3 mV; in comparison, the zeta-potential of W/O/W showed −20.9±0.8 mV and PM_W/O/W showed −13.8±1.5 mV (**Figure 6B**). As a result, by fabricating the single emulsions to double emulsions, the negative value of the surface charge was alleviated. In addition, the size of the PM_O/W and PM_W/O/W showed 46.4 nm and 21.2 nm increase after 12 days. The size of the O/W and W/O/W showed 401 nm and 599 nm increase after 12 days (**Figure 6C**). These results demonstrated that PM-encapsulated emulsions were more stable than empty emulsions.

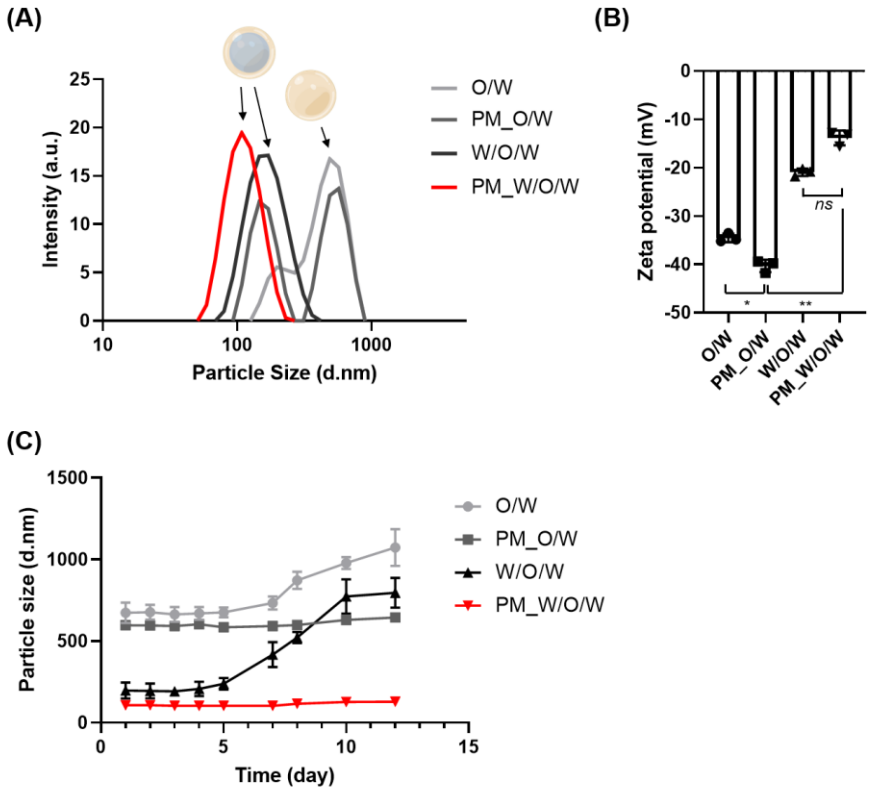

Figure 6. Characterization of emulsions using DLS. The (A) size and (B) zeta potential of O/W, PM_O/W, W/O/W, and PM_W/O/W was measured. (C) The stability of each emulsion was evaluated over 12 days. (Data are presented as the mean±SD, n=3, and p-values were calculated using one-way ANOVA. ns, not significant; *p < 0.05; **p < 0.01) (The illustration was created using Biorender)

In addition, the stability on particular environment of PM_W/O/W was assessed by comparing the size and zeta potential for 10 days. As depicted in **Figure 7**, the particle size of the PM_W/O/W maintained within a deviation of 20 nm in physiological pH and temperature over time.

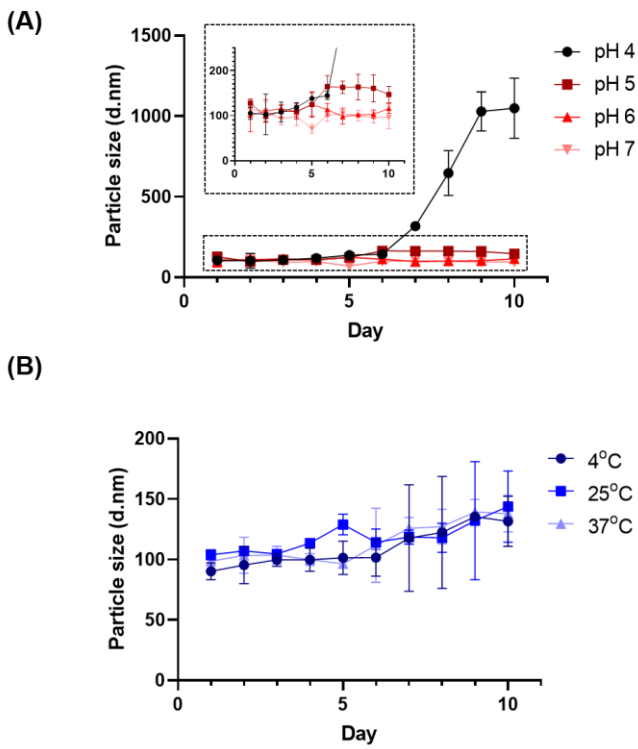

Figure 7. The particular stability of PM_W/O/W was investigated under various conditions. The change in particle size was estimated under different (A) pH and (B) temperatures for 10 days.

TEM image reveals that a biphasic structure of W/O/W and PM_W/O/W were successfully formulated in the nanoparticles (**Figure 8**). The W/O/W showed an unstable aqueous core and oil shell interface; while the PM_W/O/W showed a stable interface layer. In previous studies, the unique steric stabilization of microemulsion was made due to the localization of polyphenol at the interface between the water phase and oil phase of the emulsion [33, 46, 47]. According to these results, we deduced that the polyphenols were localized at the interface of the water phase and oil phase of the microemulsion [14, 16−19]. Therefore, we assumed that the maximum amount of encapsulated polyphenols could not exceed the localization limits. In addition, considering the autofluorescent at 405 nm excitation of polyphenol, the CLSM image showed that the PM was localized at the interface of the water phase and oil phase **(Figure 9)** [48].

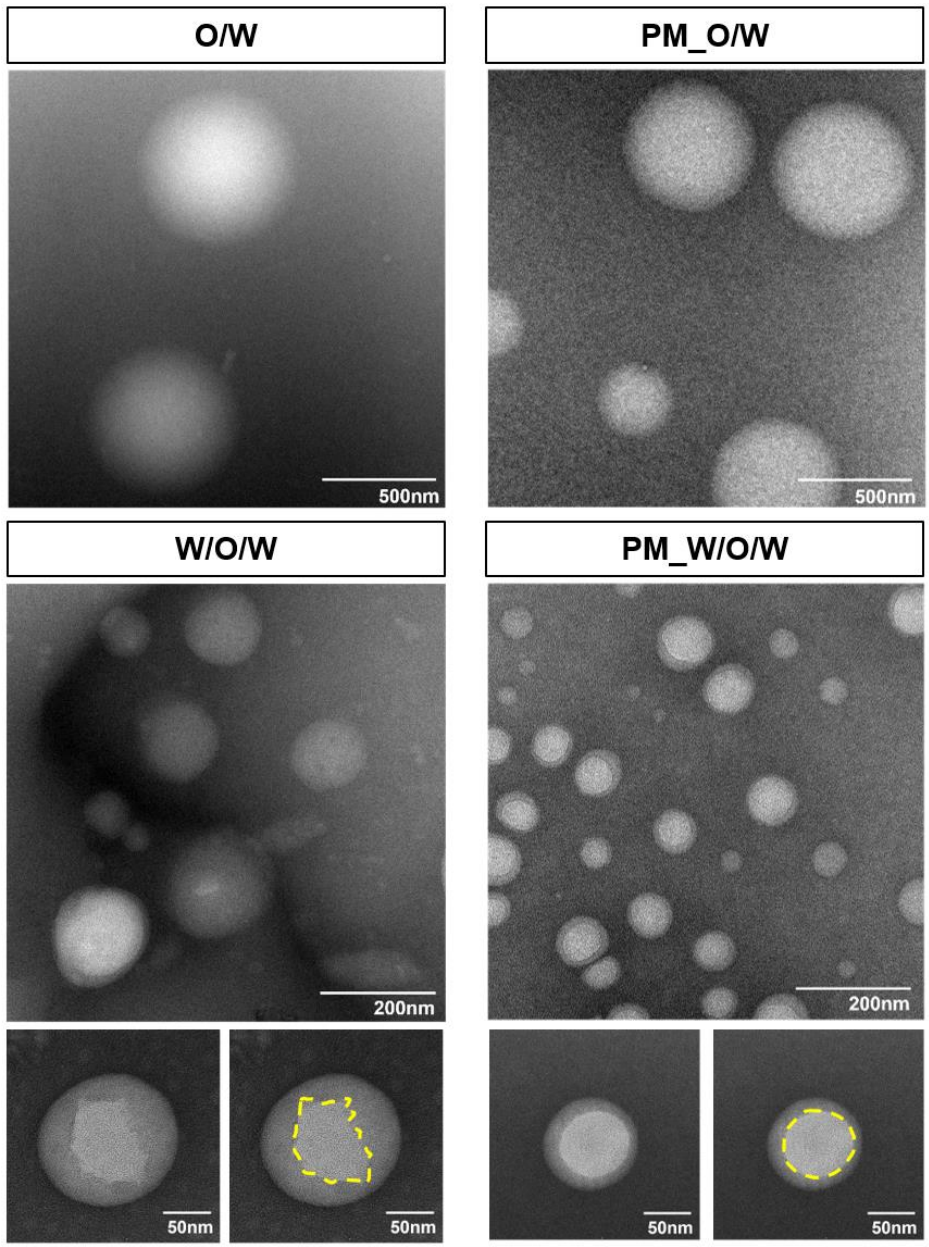

Figure 8. TEM images of emulsions proved that the double emulsion was successfully fabricated. The scale bar of O/W and PM_O/W was 500 nm, and the scale bar of W/O/W and PM_W/O/W was 200 nm.

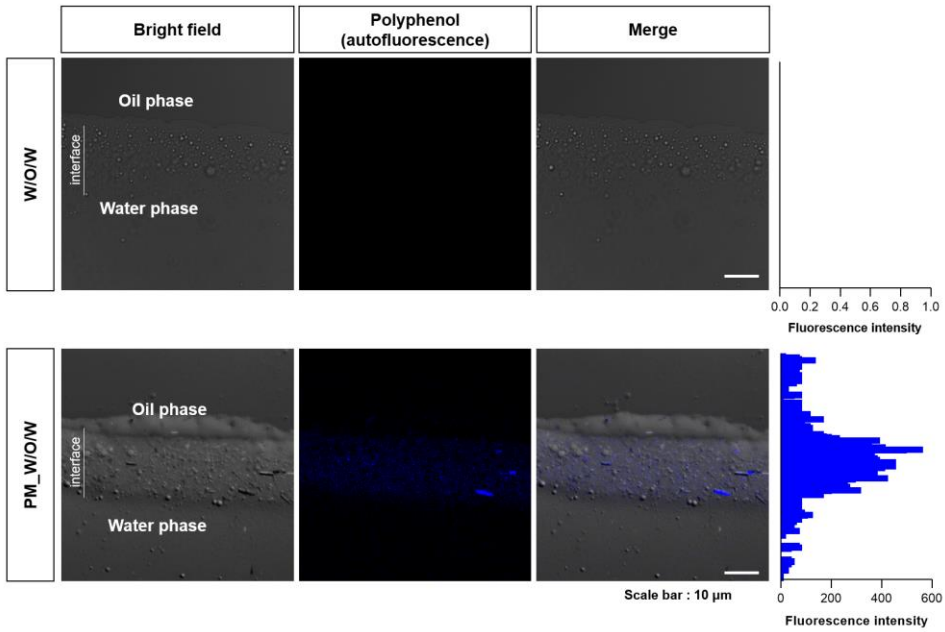

Figure 9. Confocal laser scanning microscope (CLSM) image of water phase and oil phase interface of PM_W/O/W.

Cytotoxicity of W/O/W and PM_W/O/W was confirmed by the cellular responsibility. W/O/W and PM_W/O/W showed 98.7±0.6% and 98.2±0.5% of cell viability, respectively (**Figure 10A**). Additionally, the PM_W/O/W (111.4±6.2%) display similar anti-degranulation ability with PM (100±6.5%); while W/O/W showed much more relative β-hexosaminidase release with 203.21±24.4% (**Figure 10B**). As a result, we estimated that W/O/W was effective in only transdermally delivering the PM for alleviating the inflammatory response.

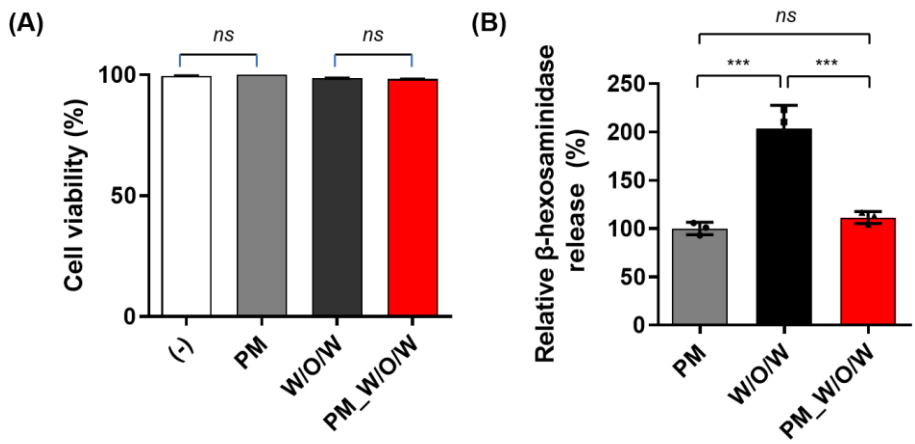

Figure 10. (A) Cell viability of PM, W/O/W and PM_W/O/W was quantified by Live/Dead assay on the HaCaT cell line. (B) To prove the anti-allergic effect of PM with double emulsion, the relative release level of β-hexosaminidase was quantified. (Data are presented as the mean±SD, n=3, and p-values were calculated using one-way ANOVA. ns, not significant; ***$p < 0.001$)

3.5. Clinical observation for AD symptoms *in vivo* model

To estimate the allergy alleviation effect of PM_W/O/W on the *in vivo* AD mice model, we used DNCB as allergens in BALB/c mice (**Figure 11A**). As shown in **Figure 11B**, AD was effectively induced by DNCB. AD-related symptoms like hyperkeratosis and dryness, and redness on DNCB-treated skin of sham group demonstrated that AD was successfully induced in the mice model. We demonstrated that treatment with PM_W/O/W attenuates the severity of AD by clinical observation, such as dermatitis score and relative ear thickness which indicated the severity of AD symptoms.

To investigate the retention of double emulsions within the skin, we obtained the IVIS images using the dye-encapsulated double emulsion. The Nile red was used as the dye due to the its similar molar weight and hydrophobicity with polyphenols. As shown in **Figure 12**, we verified that the double emulsions transdermally delivered after 24 h, considering the 65% decrease in radiant efficiency compared to 1 h after treatment. Thus, in this study, the treatment period of the sample was designed with 48 h and 72 h to prevent the overdose of drugs.

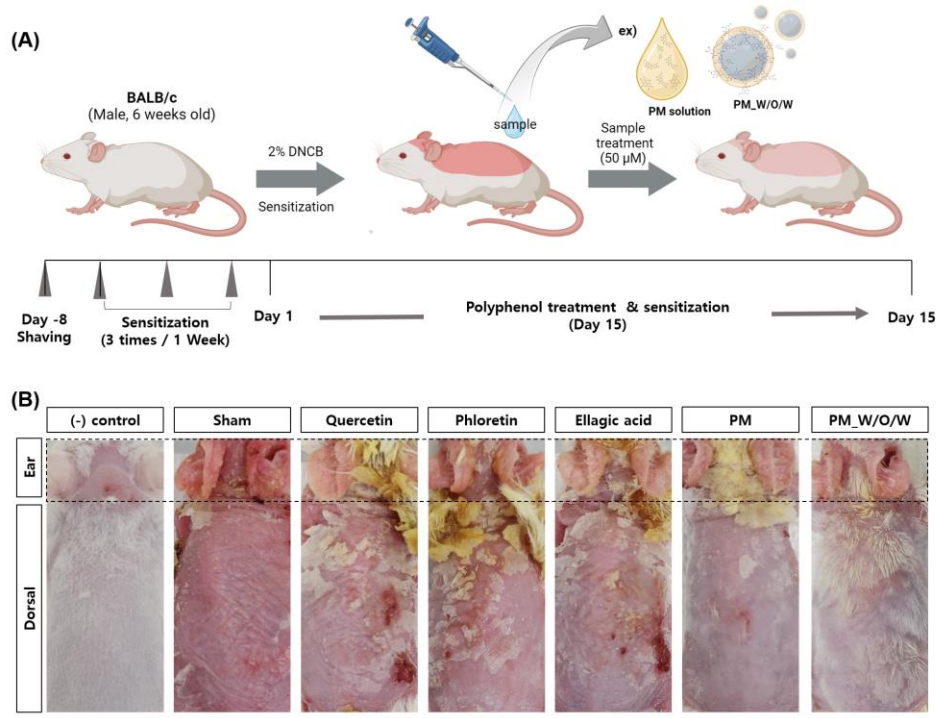

Figure 11. (A) The overall timeline of *in vivo* experiment with DNCB-induced atopic dermatitis (AD) mice model. The illustration was created using Biorender. (B) was the optical observations of AD-induced skin from ear to dorsal of each group.

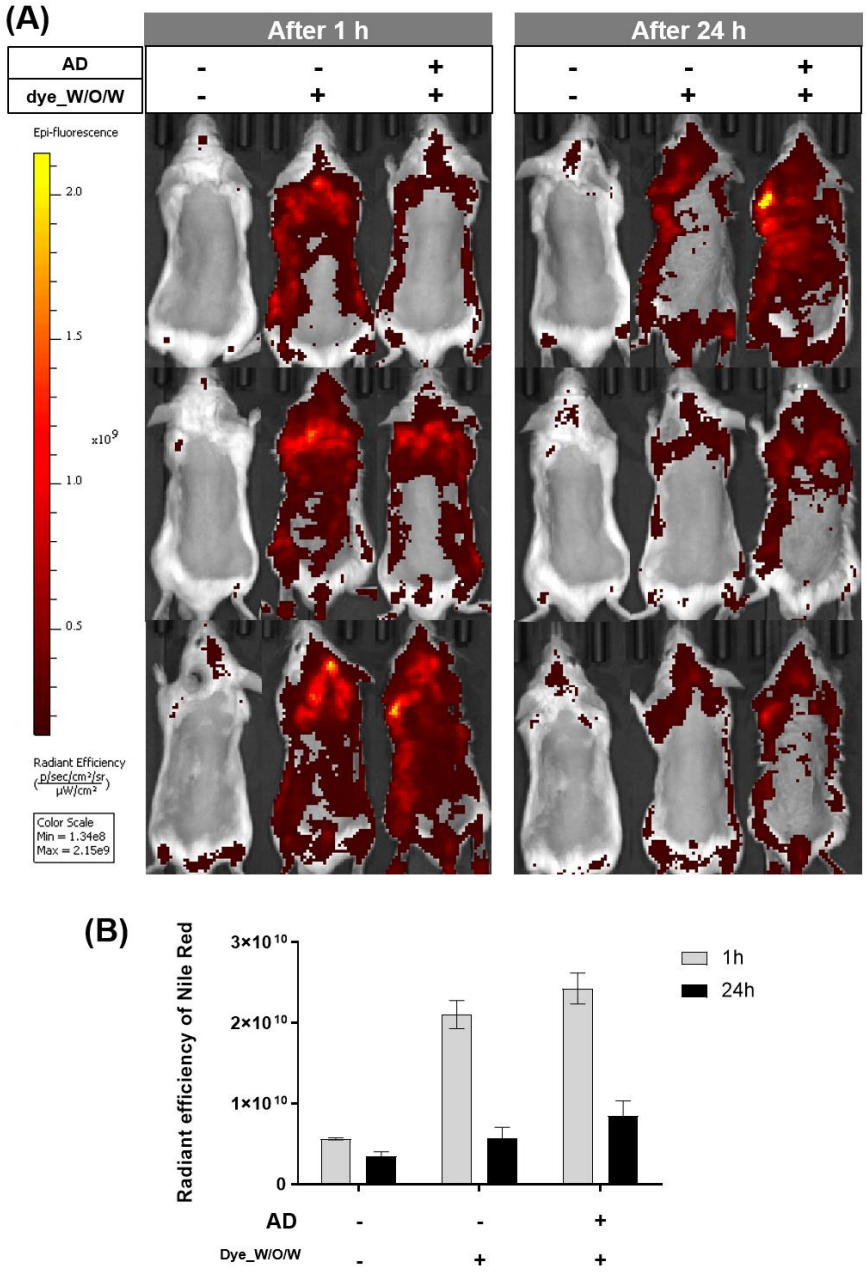

Figure 12. (A) The retention time of nanoparticles was estimated using the dye-encapsulated double emulsion by IVIS images. (B) The quantified value of radiant efficiency of the double emulsion was calculated based on the IVIS images.

In addition, the *in vivo* toxicity of PM and PM_W/O/W was measured with irritation analysis by calculating the erythema index. As seen in **Figure 13**, the possibility of toxicity by PM and PM_W/O/W was negligible according to little significant change in erythema index after 1 h and 24 h. Moreover, considering the controlled release efficiency of the emulsion system, we surmised that sustained release of PM would reduce toxicity induced by the overdose or localization of drugs at the epidermis [49].

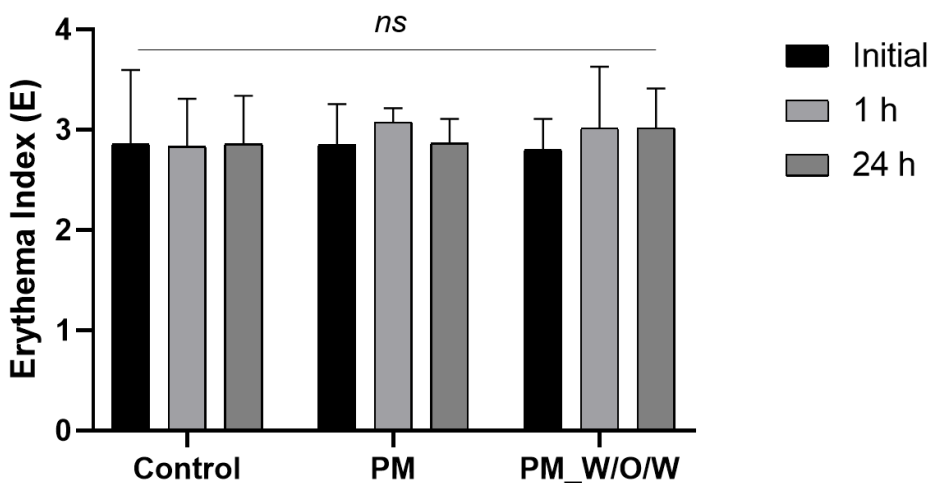

Figure 13. The *in vivo* toxicity of PM and PM_W/O/W was estimated with the irritation analysis.

During the experiment, the dermatitis score was maintained between 8 and 10 in the sham group; while the negative control group showed between 0 and 1, which indicated the healthy normal skin. The PM_W/O/W alleviated the skin condition with the lowest dermatitis score of 5 compared to Q (score from 10.3 to 9), P (score from 10.7 to 11), E (score from 10 to 9.3), PM (score from 8.7 to 6.3) (**Figure 14A**). Especially, the dermatitis score of the PM_W/O/W mice was 5 on the last day of experiment; while PM has 7.67, Q has 9, P has 11, E has 9.3, negative control group has 0.67, and sham group has 9 (**Figure 14B**).

Additionally, we measured the ear thickness by using a digital caliper on days 3, 5, 10, and 15. Excessive inflammatory reactions occur on the AD-induced skin, resulting in swelling and edema, which increase the thickness of the ears and paws [39-41]. As shown in **Figures 14C and 14D**, the relative ear thickness slowly increased in all AD-induced groups; however, PM_W/O/W treated group had the lowest thickness (166.2± 7.8%) compared to single polyphenol and PM-treated groups on the last day. The sham group showed 208.9±0.8% of highly increased ear thickness. Although the higher value than the PM_W/O/W treated group, the PM treated group showed relatively less increase in ear thickness of 185±16.5% than single polyphenols treated groups; 193±23.3% in Q, 200.5±6.7% in P, and 202.3±39.6% in E. Therefore, these results proved that the PM_W/O/W efficiently alleviated the symptoms of AD compared to single polyphenols and PM.

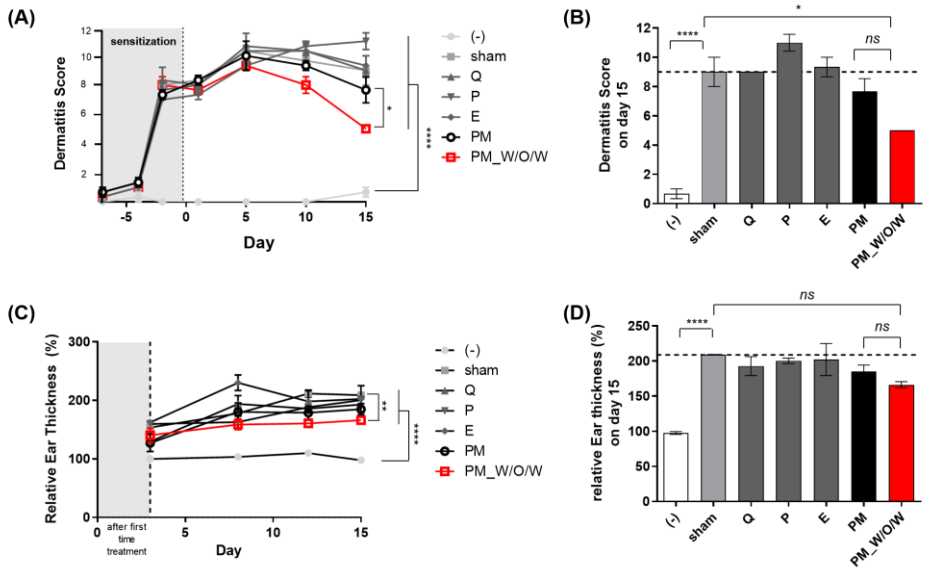

Figure 14. (A) The dermatitis score was quantified by adding the value of each symptom, including erythema/hemorrhage, scarring/dryness, edema, and excoriation/erosion during the experiments. (B) was the dermatitis score on the last day of the experiment (day 15). (C) Ear thickness was analyzed by relative value based on the negative control group on the same day, considering the individual measurement errors with digital calipers. (D) also was the relative ear thickness on the last day of the experiment. (Data are presented as the mean±SD, n = 3, and p-values were calculated using one-way ANOVA, and two-way ANOVA. ns, not significant; $*p < 0.05$; $**p < 0.01$; $****p < 0.0001$.)

3.6. Histological analysis of alleviation of AD

To investigate the anti-allergic effect, we employed histological analysis of AD-induced dorsal and ear skins. Because of the hyperkeratosis and hyperplasia of AD-induced skin, the dermal and epidermal thickness is increased. To assess the severity of AD, we measured the dermal thickness, epidermal thickness, and ear thickness by H&E staining images (**Figures 15A and 16A**).

The epidermal thickness of the sham group was 107.1±25.4 ㎛, which was thicker than the native epidermal thickness of the negative control group, measured at 16.7±1.9 ㎛. The epidermal thickness of PM_W/O/W mostly less increased with 54.6±3.8 ㎛; while the epidermal thickness of Q, P, E, and PM treated groups was 114.6±18.4 ㎛, 114.4±21.3 ㎛, 91.5±8.4 ㎛, and 84.1±21.6 ㎛. In addition, the dermal thickness of the sham group was 454.4±18 ㎛, while the native dermal thickness of the negative control group was 362.7±13.2 ㎛ (**Figure 15B**). The dermal thickness of PM_W/O/W mostly less increased with 396.6±22.3 ㎛; while the dermal thickness of Q, P, E, and PM treated groups was 436.6±21.2 ㎛, 533±99.2 ㎛, 464.4±24.5 ㎛, and 437.7±48.6 ㎛ (**Figure 15C**).

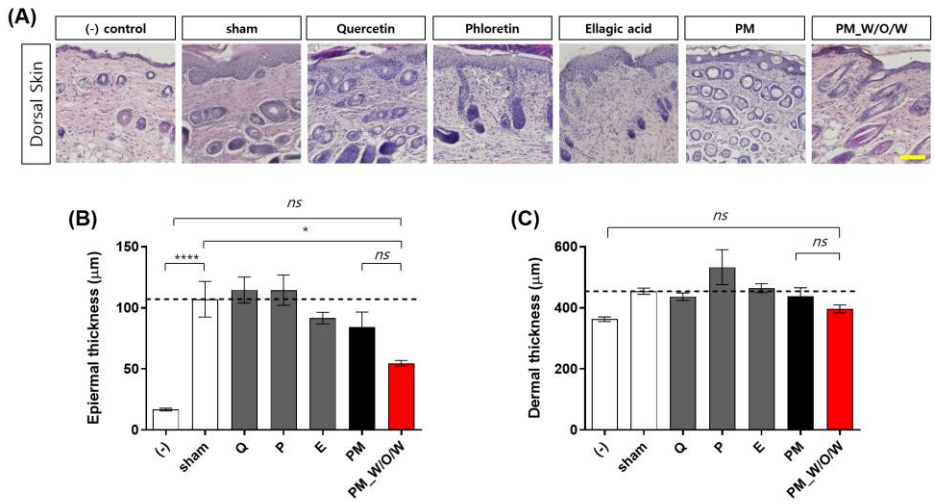

Figure 15. Histological analysis of mice dorsal skin lesions. (A) was the image of hematoxylin and eosin (H&E) staining. The scale bar was 100 μm. (B–C) Epidermal thickness and dermal thickness were measured based on the H&E stained image using Image J software. (Data are presented as the mean±SD, n=3, and p–values were calculated using one–way ANOVA. ns, not significant; $*p < 0.05$; $****p < 0.0001$)

Additionally, the ear thickness was also quantified based on the H&E images (**Figure 16A**). The ear thickness of the sham was 422.3±21 μm, and the native ear thickness of the negative control group was 200.7 ±40.8 μm. The PM_W/O/W showed the most mitigated AD symptoms with 318.5±25.7 μm, respectively. The ear thickness of Q, P, and E showed 340.5±10.5 μm, 340±19.8 μm, and 354.5±46.3 μm (**Figure 16B**). These results about skin thickness demonstrated that the PM_W/O/W had a remarkable AD alleviation effect compared to single polyphenols and PM.

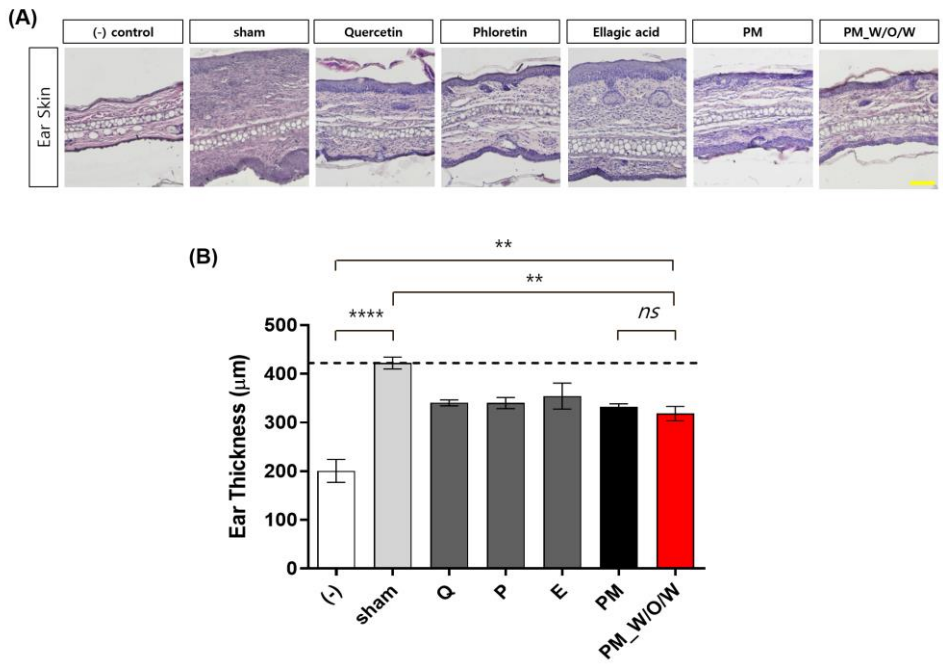

Figure 16. Histological analysis of mice ear skin lesions. (A) was the image of hematoxylin and eosin (H&E) staining. The scale bar was 100 μm. (B) Ear thickness was measured based on the H&E stained image using Image J software. (Data are presented as the mean±SD, n=3, and p-values were calculated using one-way ANOVA. ns, not significant; **p < 0.01; ****p < 0.0001)

3.7. Immunological analysis of AD response

To evaluate the anti-allergic effect on immune response, inflammatory cell infiltration beneath the dermis and hypodermis was stained by toluidine blue (**Figure 17A**). Mast cells were stained purple and the background was stained blue. As shown in **Figure 17B**, the number of mast cells was 20.3±2 cells/mm^2 in the sham group while the native number of mast cells was 7.3±2.8 cells/mm^2 in the negative control group. Especially, the PM_W/O/W treated group represented less number of mast cells with 10.8±3.7 cells/mm^2 compared to single polyphenols and PM treated groups, respectively. The Q, P, E, and PM treated group showed 20.6±2.6 cells/mm^2, 28.3±10.6 cells/mm^2, 25.8±10.1 cells/mm^2, and 18.6 ±10.8 cells/mm^2 of mast cells in dermis and hypodermis.

In addition, we measured the serum IgE level as a systemic biomarker of AD. The sham group showed the serum IgE level with 48.6± 3.46 ng/mL compared to negative control groups (27.4±1.6 ng/mL). PM_W/O/W treated group represented the lowest level of serum IgE with 29.7±1.5 ng/mL compared to single polyphenols and PM treated group, respectively. The Q treated group has 38.2±5.4 ng/mL, P treated group has 45.3±14.3 ng/mL, E treated group has 47.8±10.5 ng/mL, and PM has 33.5±6.7 ng/mL of serum IgE level (**Figure 18**). Therefore, the reduction of inflammatory cell infiltration and serum IgE level in the PM_W/O/W treated group demonstrated that our ratio of PM and double emulsion transdermal delivery carrier induced the most effective AD.

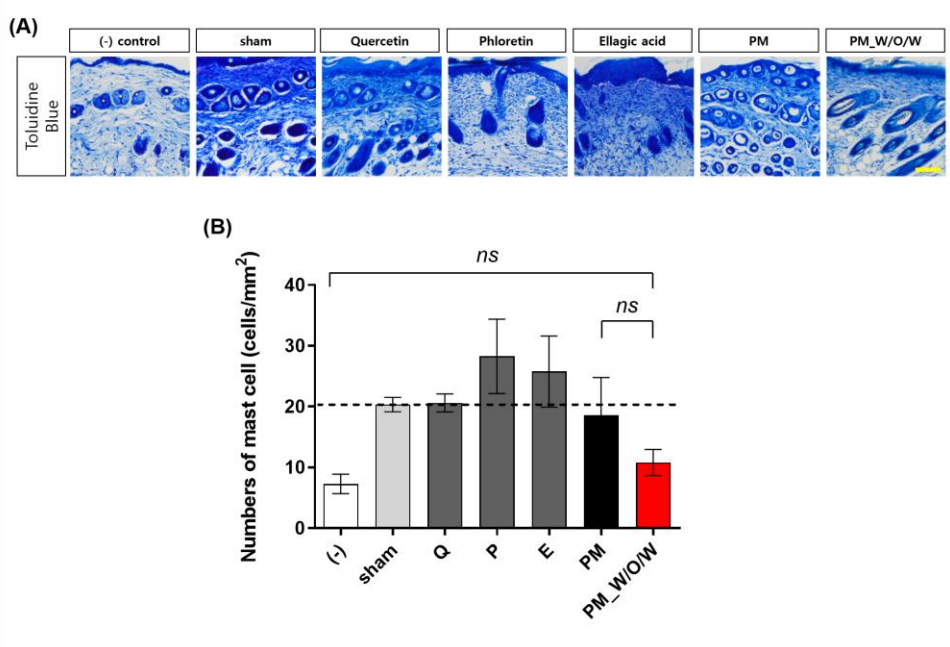

Figure 17. Immunological analysis of mice dorsal skin lesions. (A) was the image of toluidine blue staining. (B) Mast cells that were stained purple were counted beneath the dermis and hypodermis. The scale bar was 100 μm. (Data are presented as the mean±SD, n = 3, p-values were calculated using one-way ANOVA. ns, not significant)

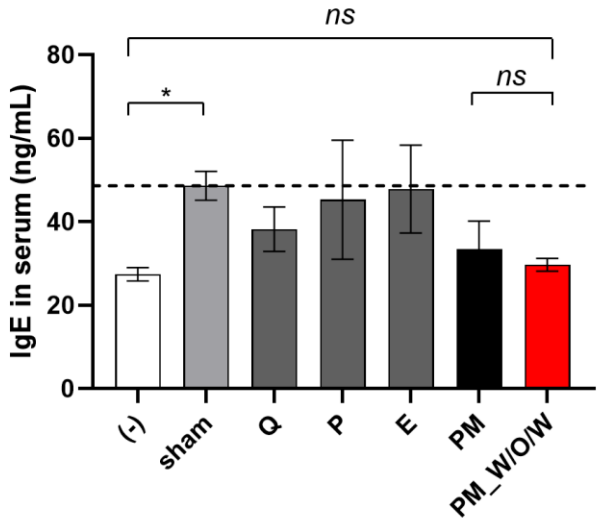

Figure 18. Immunological analysis of *in vivo* AD-induced mice model. (A) The serum IgE level was estimated using ELISA. (Data are presented as the mean±SD, n = 3, p-values were calculated using one-way ANOVA. ns, not significant; $*p < 0.05$)

Chapter 4. Conclusion

Herein, we screened an specific composition and ratio of polyphenol mixture (PM)-based therapeutic system for atopic dermatitis (AD). We suggested the optimal ratio of PM using specific polyphenols; quercetin (Q), phloretin (P), and ellagic acid (E). Although there are many biological efficiency of polyphenols, polyphenol shows some limitations such as the susceptibility to oxidation, low bioavailability, and low stability to be used as a component of products. Therefore, to enhance the bioavailability and transdermal delivery efficiency of polyphenols, we used a double emulsion (W/O/W) as a nanocarrier in this study. In particular, the W/O/W which is the nanocarrier of the transdermal drug delivery system was fabricated, and we proved the improved polyphenol encapsulation efficiency and stability. Finally, we induced AD with DNCB in BALB/c mice and demonstrated that PM_W/O/W could alleviate the AD with clinical, histological, and immunological analysis. According to the enhanced AD alleviation effect of PM compared to single polyphenols, we can represent that the PM had a synergetic effect at the relatively high total polyphenol concentration (50 μM) where a single polyphenol showed side effects. Moreover, PM_W/O/W showed a remarkable reconstruction of the skin physiology compared to other groups *in vivo*. According to these results, we proved that the anti-allergic effect of PM_W/O/W was caused by not only the PM but also the efficient delivery of the nanocarrier, W/O/W. Therefore, we could suggest new insights into the combinational

therapy of polyphenols and also be applied in the transdermal delivery system for other disease models.

Supporting Information

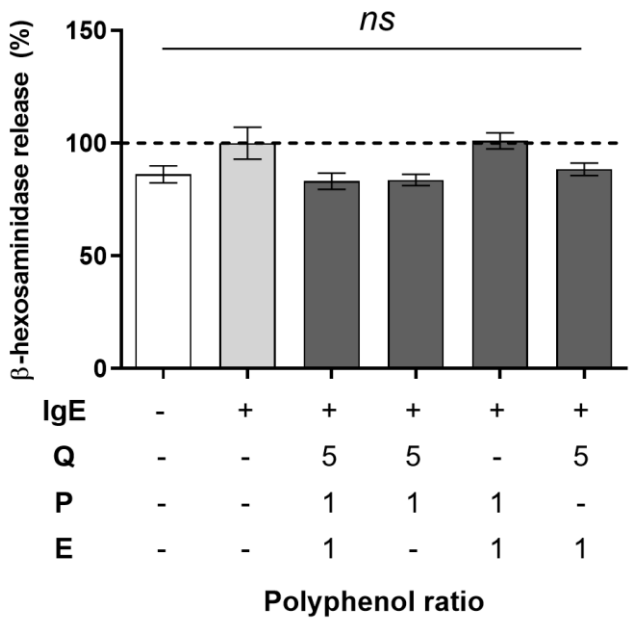

Figure S1. The β-hexosaminidase assay was confirmed the anti-allergic effect of PM by comparing the different polyphenol mixtures, which composed of two types of polyphenol. (Data are presented as the mean±SD, n=3, and p-values were calculated using one-way ANOVA. ns, not significant)

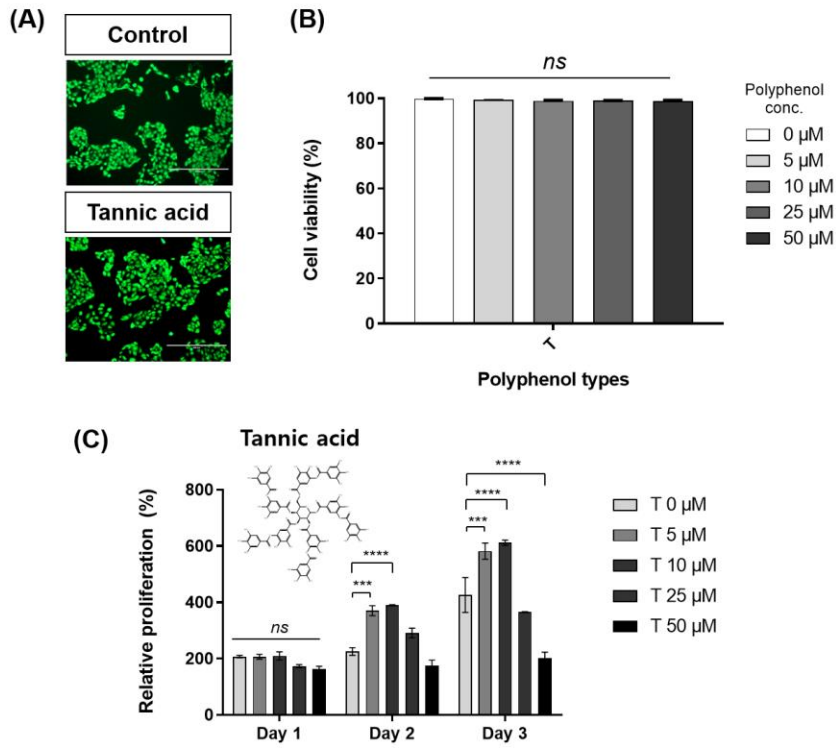

Figure S2. The influence of tannic acid (T, other types of polyphenol) was confirmed by investigating the cellular response in HaCaT cells. (A–B) showed the cell viability of T–treated cells by Live/Dead assay. (C) Cell proliferation of T–treated cells showed by CCK–8 assay. (Data are presented as the mean±SD, n=3, and p–values were calculated using one–way ANOVA, and two–way ANOVA. ns, not significant; *$p < 0.05$; ***$p < 0.001$; ****$p < 0.0001$.)

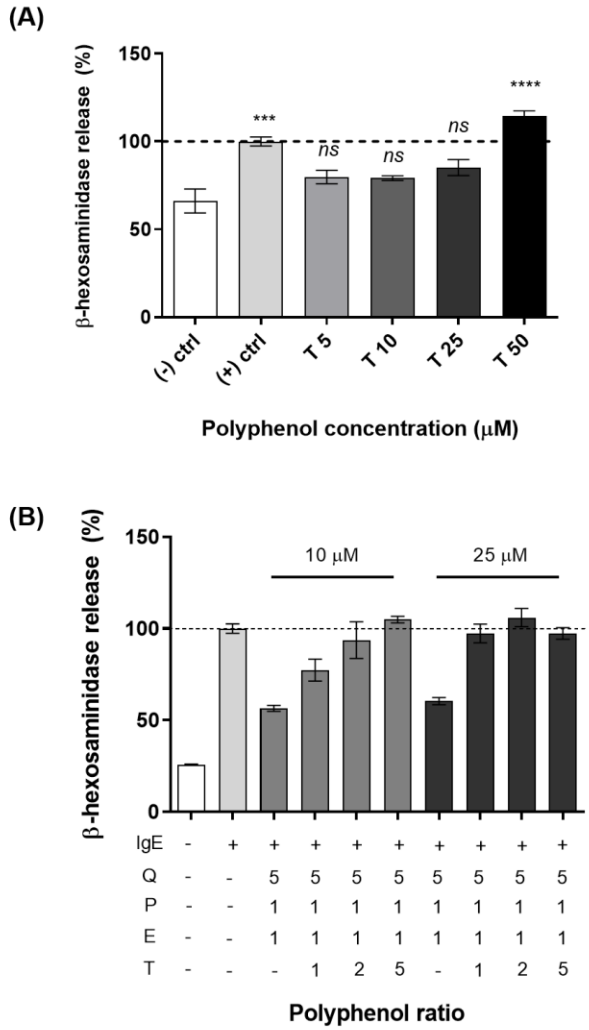

Figure S3. (A) The anti-allergic efficacy of T was investigated by β-hexosaminidase assay in IgE-sensitized RBL-2H3 cells. (B) showed the comparison of the anti-allergic effect of different total polyphenol concentrations and composition of PM in IgE-sensitized RBL-2H3 cells. (Data are presented as the mean±SD, n=3, and p-values were calculated using one-way ANOVA. ns, not significant; ***$p < 0.001$; ****$p < 0.0001$).

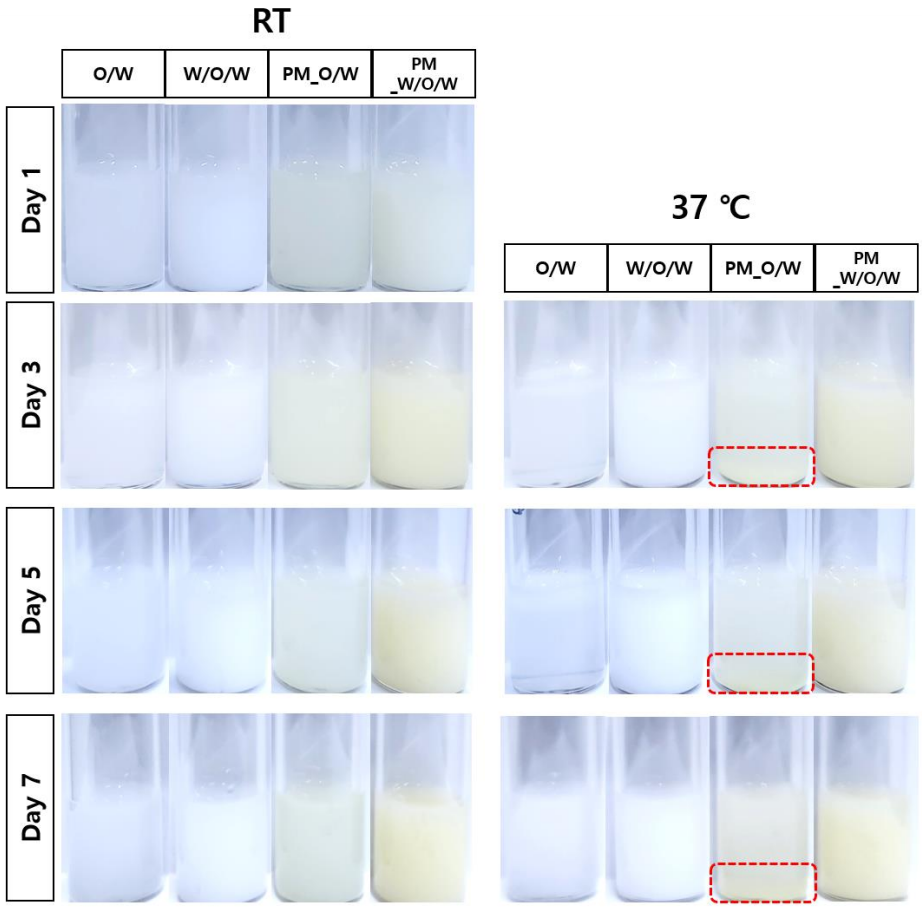

Figure S4. The optical image of single emulsions (O/W and PM_O/W) and double emulsions (W/O/W and PM_W/O/W) was obtained on days 1, 3, 5, and 7 at room temperature and 37 ℃.

Bibliography

[1] S.C. Dharmage, A. Lowe, M.C. Matheson, J. Burgess, K. Allen, M.J. Abramson, Atopic dermatitis and the atopic march revisited, Allergy 69(1) (2014) 17-27.
[2] A.M. Drucker, A.R. Wang, W.-Q. Li, E. Sevetson, J.K. Block, A.A. Qureshi, The burden of atopic dermatitis: summary of a report for the National Eczema Association, Journal of Investigative Dermatology 137(1) (2017) 26-30.
[3] T. Zheng, J. Yu, M.H. Oh, Z. Zhu, The atopic march: progression from atopic dermatitis to allergic rhinitis and asthma, Allergy, asthma & immunology research 3(2) (2011) 67-73.
[4] N.A. Gandhi, B.L. Bennett, N.M. Graham, G. Pirozzi, N. Stahl, G.D. Yancopoulos, Targeting key proximal drivers of type 2 inflammation in disease, Nature reviews Drug discovery 15(1) (2016) 35-50.
[5] L.F. Ariëns, D.S. Bakker, J. van der Schaft, F.M. Garritsen, J.L. Thijs, M.S. de Bruin-Weller, Dupilumab in atopic dermatitis: rationale, latest evidence and place in therapy, Therapeutic Advances in Chronic Disease 9(9) (2018) 159-170.
[6] A. Chu, N. Devasenapathy, M. Wong, A. Srivastava, R. Ceccacci, C. Lin, D. Chu, CANCER RISK WITH TOPICAL PIMECROLIMUS AND TACROLIMUS FOR ATOPIC DERMATITIS: SYSTEMATIC REVIEW AND BAYESIAN META-ANALYSIS, Annals of Allergy, Asthma & Immunology 129(5) (2022) S7.
[7] J.M. Hanifin, M.R. Ling, R. Langley, D. Breneman, E. Rafal, T.O.S. Group, Tacrolimus ointment for the treatment of atopic dermatitis in adult patients: part I, efficacy, Journal of the American Academy of Dermatology 44(1) (2001) S28-S38.
[8] P. Nghiem, G. Pearson, R.G. Langley, Tacrolimus and pimecrolimus: from clever prokaryotes to inhibiting calcineurin and treating atopic dermatitis, Journal of the American Academy of Dermatology 46(2) (2002) 228-241.
[9] T. Ruzicka, T. Bieber, E. Schöpf, A. Rubins, A. Dobozy, J.D. Bos, S. Jablonska, I. Ahmed, K. Thestrup-Pedersen, F. Daniel, A short-term trial of tacrolimus ointment for atopic dermatitis, New England Journal of Medicine 337(12) (1997) 816-821.
[10] A.S. Paller, P. Mina-Osorio, F. Vekeman, S. Boklage, U.G. Mallya, S. Ganguli, M. Kaur, M.-N. Robitaille, E.C. Siegfried, Prevalence of type 2 inflammatory diseases in pediatric patients with atopic dermatitis: Real-world evidence, Journal of the American Academy of Dermatology 86(4) (2022) 758-765.
[11] I.A. Deckers, S. McLean, S. Linssen, M. Mommers, C. Van Schayck, A. Sheikh, Investigating international time trends in the incidence and prevalence of atopic eczema 1990–2010: a systematic review of epidemiological studies, PloS one 7(7) (2012) e39803.

[12] S. Sharma, A.S. Naura, Potential of phytochemicals as immune-regulatory compounds in atopic diseases: A review, Biochemical Pharmacology 173 (2020) 113790.
[13] S. Wu, Y. Pang, Y. He, X. Zhang, L. Peng, J. Guo, J. Zeng, A comprehensive review of natural products against atopic dermatitis: Flavonoids, alkaloids, terpenes, glycosides and other compounds, Biomedicine & Pharmacotherapy 140 (2021) 111741.
[14] Y. Zhou, J. Zheng, Y. Li, D.-P. Xu, S. Li, Y.-M. Chen, H.-B. Li, Natural polyphenols for prevention and treatment of cancer, Nutrients 8(8) (2016) 515.
[15] J.A. Nichols, S.K. Katiyar, Skin photoprotection by natural polyphenols: anti-inflammatory, antioxidant and DNA repair mechanisms, Archives of dermatological research 302 (2010) 71-83.
[16] S. Suk, G.T. Kwon, E. Lee, W.J. Jang, H. Yang, J.H. Kim, N. Thimmegowda, M.Y. Chung, J.Y. Kwon, S. Yang, Gingerenone A, a polyphenol present in ginger, suppresses obesity and adipose tissue inflammation in high-fat diet-fed mice, Molecular nutrition & food research 61(10) (2017) 1700139.
[17] A. Kutan Fenercioglu, T. Saler, E. Genc, H. Sabuncu, Y. Altuntas, The effects of polyphenol-containing antioxidants on oxidative stress and lipid peroxidation in Type 2 diabetes mellitus without complications, Journal of endocrinological investigation 33 (2010) 118-124.
[18] E. Torre, Molecular signaling mechanisms behind polyphenol-induced bone anabolism, Phytochemistry Reviews 16(6) (2017) 1183-1226.
[19] C.C. Tangney, H.E. Rasmussen, Polyphenols, inflammation, and cardiovascular disease, Current atherosclerosis reports 15 (2013) 1-10.
[20] Y.-R. Liao, J.-Y. Lin, Quercetin intraperitoneal administration ameliorates lipopolysaccharide-induced systemic inflammation in mice, Life sciences 137 (2015) 89-97.
[21] R. Kleemann, L. Verschuren, M. Morrison, S. Zadelaar, M.J. van Erk, P.Y. Wielinga, T. Kooistra, Anti-inflammatory, anti-proliferative and anti-atherosclerotic effects of quercetin in human in vitro and in vivo models, Atherosclerosis 218(1) (2011) 44-52.
[22] M.P. Nair, C. Kandaswami, S. Mahajan, K.C. Chadha, R. Chawda, H. Nair, N. Kumar, R.E. Nair, S.A. Schwartz, The flavonoid, quercetin, differentially regulates Th-1 (IFNγ) and Th-2 (IL4) cytokine gene expression by normal peripheral blood mononuclear cells, Biochimica et Biophysica Acta (BBA)-Molecular Cell Research 1593(1) (2002) 29-36.
[23] C.-S. Wu, S.-C. Lin, S. Li, Y.-C. Chiang, N. Bracci, C.W. Lehman, K.-T. Tang, C.-C. Lin, Phloretin alleviates dinitrochlorobenzene-induced dermatitis in BALB/c mice, International Journal of Immunopathology and Pharmacology 34 (2020) 2058738420929442.
[24] W.-C. Huang, Y.-W. Dai, H.-L. Peng, C.-W. Kang, C.-Y. Kuo, C.-J. Liou, Phloretin ameliorates chemokines and ICAM-1 expression via blocking of the NF-κB pathway in the TNF-α-induced HaCaT human keratinocytes, International Immunopharmacology 27(1) (2015) 32-37.

[25] T.-Y. Gil, C.-H. Hong, H.-J. An, Anti-inflammatory effects of ellagic acid on keratinocytes via MAPK and STAT pathways, International Journal of Molecular Sciences 22(3) (2021) 1277.
[26] L. Ma, M. Kohli, A. Smith, Nanoparticles for combination drug therapy, ACS nano 7(11) (2013) 9518-9525.
[27] W. Sun, P.E. Sanderson, W. Zheng, Drug combination therapy increases successful drug repositioning, Drug discovery today 21(7) (2016) 1189-1195.
[28] T. Möttönen, P. Hannonen, M. Leirisalo-Repo, M. Nissilä, H. Kautiainen, M. Korpela, L. Laasonen, H. Julkunen, R. Luukkainen, K. Vuori, Comparison of combination therapy with single-drug therapy in early rheumatoid arthritis: a randomised trial, The Lancet 353(9164) (1999) 1568-1573.
[29] J. Mao, M.S. Gold, Combination drug therapy for chronic pain: a call for more clinical studies, The Journal of Pain 12(2) (2011) 157-166.
[30] M.J. Lawrence, G.D. Rees, Microemulsion-based media as novel drug delivery systems, Advanced drug delivery reviews 64 (2012) 175-193.
[31] T. Hoar, J. Schulman, Transparent water-in-oil dispersions: the oleopathic hydro-micelle, Nature 152(3847) (1943) 102-103.
[32] M.R. Islam, S. Uddin, M.R. Chowdhury, R. Wakabayashi, M. Moniruzzaman, M. Goto, Insulin transdermal delivery system for diabetes treatment using a biocompatible ionic liquid-based microemulsion, ACS Applied Materials & Interfaces 13(36) (2021) 42461-42472.
[33] M. Jalali-Jivan, F. Garavand, S.M. Jafari, Microemulsions as nano-reactors for the solubilization, separation, purification and encapsulation of bioactive compounds, Advances in colloid and interface science 283 (2020) 102227.
[34] S. Saffarionpour, One-step preparation of double emulsions stabilized with amphiphilic and stimuli-responsive block copolymers and nanoparticles for nutraceuticals and drug delivery, JCIS Open 3 (2021) 100020.
[35] I.D. Rosca, F. Watari, M. Uo, Microparticle formation and its mechanism in single and double emulsion solvent evaporation, Journal of controlled release 99(2) (2004) 271-280.
[36] B. Lu, Y. Bo, M. Yi, Z. Wang, J. Zhang, Z. Zhu, Y. Zhao, J. Zhang, Enhancing the Solubility and Transdermal Delivery of Drugs Using Ionic Liquid-In-Oil Microemulsions, Advanced Functional Materials 31(34) (2021) 2102794.
[37] J. Andrade, M. Corredig, Vitamin D3 and phytosterols affect the properties of polyglycerol polyricinoleate (PGPR) and protein interfaces, Food Hydrocolloids 54 (2016) 278-283.
[38] K. Urban, G. Wagner, D. Schaffner, D. Röglin, J. Ulrich, Rotor-stator and disc systems for emulsification processes, Chemical Engineering & Technology: Industrial Chemistry-Plant Equipment-Process Engineering-Biotechnology 29(1) (2006) 24-31.
[39] S.-E. Son, S.-J. Park, J.-M. Koh, D.-S. Im, Free fatty acid receptor 4 (FFA4) activation ameliorates 2, 4-dinitrochlorobenzene-induced atopic dermatitis by increasing regulatory T cells in mice, Acta Pharmacologica Sinica 41(10) (2020) 1337-1347.

[40] H.-Y. Jang, J.-H. Koo, S.-M. Lee, B.-H. Park, Atopic dermatitis-like skin lesions are suppressed in fat-1 transgenic mice through the inhibition of inflammasomes, Experimental & Molecular Medicine 50(6) (2018) 1-9.
[41] K.-J. Lee, K.P. Ulrich N'deh, G.-J. Kim, J.W. Choi, J. Kim, E.-K. Kim, J.H. An, Fe2+ : Fe3+ Molar Ratio Influences the Immunomodulatory Properties of Maghemite (ɣ-Fe2O3) Nanoparticles in an Atopic Dermatitis Model, ACS Applied Bio Materials 4(2) (2021) 1252-1267.
[42] M.S. Matos, R. Romero-Díez, A. Álvarez, M. Bronze, S. Rodríguez-Rojo, R.B. Mato, M. Cocero, A.A. Matias, Polyphenol-rich extracts obtained from winemaking waste streams as natural ingredients with cosmeceutical potential, Antioxidants 8(9) (2019) 355.
[43] S. Liu, W. Jiang, C. Liu, S. Guo, H. Wang, X. Chang, Chinese chestnut shell polyphenol extract regulates the JAK2/STAT3 pathway to alleviate high-fat diet-induced, leptin-resistant obesity in mice, Food & Function 14(10) (2023) 4807-4823.
[44] A.K. Ghosh, N.E. Kay, C.R. Secreto, T.D. Shanafelt, Curcumin inhibits prosurvival pathways in chronic lymphocytic leukemia B cells and may overcome their stromal protection in combination with EGCG, Clinical Cancer Research 15(4) (2009) 1250-1258.
[45] A. Saha, T. Kuzuhara, N. Echigo, M. Suganuma, H. Fujiki, New Role of (−)-Epicatechin in Enhancing the Induction of Growth Inhibition and Apoptosis in Human Lung Cancer Cells by CurcuminEC Enhances the Effects of Curcumin, Cancer prevention research 3(8) (2010) 953-962.
[46] M. Zembyla, B.S. Murray, A. Sarkar, Water-in-oil Pickering emulsions stabilized by water-insoluble polyphenol crystals, Langmuir 34(34) (2018) 10001-10011.
[47] M. Zembyla, A. Lazidis, B.S. Murray, A. Sarkar, Stability of water-in-oil emulsions co-stabilized by polyphenol crystal-protein complexes as a function of shear rate and temperature, Journal of Food Engineering 281 (2020) 109991.
[48] M. Zembyla, B.S. Murray, S.J. Radford, A. Sarkar, Water-in-oil Pickering emulsions stabilized by an interfacial complex of water-insoluble polyphenol crystals and protein, Journal of Colloid and Interface Science 548 (2019) 88-99.
[49] A. Kogan, N. Garti, Microemulsions as transdermal drug delivery vehicles, Advances in colloid and interface science 123 (2006) 369-385.

Abstract in Korean

Anti-Allergic Effect of Polyphenol Mixture in Atopic Dermatitis using Double Emulsion-Mediated Delivery

성 명(Subin Choi)
학과 및 전공(Interdisciplinary Program in Bioengineering)
The Graduate School of Engineering
Seoul National University

폴리페놀은 항염증, 항산화, 항바이러스를 포함한 다양한 생물학적 활성을 가진다. 하지만 폴리페놀은 낮은 용해도와 혼화성, 그리고 산소에 민감한 성질을 가지기 때문에, 폴리페놀을 안정화된 제형으로 사용하기 위해서는 전달하는 방법을 고려해야 한다. 본 연구에서는 아토피 피부염에 적용하기 위해 단일 폴리페놀보다 더 우수한 효과를 보이는 특정 폴리페놀, 특정 비율로 구성된 폴리페놀 혼합물을 찾았다. 또한 이중 에멀전인 water-in-oil-in-water (W/O/W) 시스템을 적용해서 폴리페놀 혼합물을 전달했다. *in vitro* 탈과립 억제 실험을 통해, 특정 몰 농도 비를 가지는 폴리페놀 혼합물 (퀴세틴:프로레틴:엘라직 액시드 = 5:1:1)을 선정했고, 이 혼합물의 치료범위를 측정했다. 또한, 폴리페놀 혼합물을 전달하는 전달체로서 단일 에멀전인 oil-in-water (O/W)에 비해 이중 에멀전이 적합함을 증명했다. *in vivo* DNCB 유도 아토피 마우스 모델에서

조직학적, 면역학적 분석을 통해, 폴리페놀 혼합물이 담지된 이중 에멀전(PM_W/O/W)이 단일 폴리페놀과 이중 에멀전에 담지 되지 않은 폴리페놀 혼합물보다 아토피 완화 효과가 뛰어남을 보여줬다. 이러한 실험 결과를 통해 특정 농도의 폴리페놀 혼합물과 이중 에멀절을 이용한 새로운 아토피 치료 시스템을 제안했으며, 다른 알레르기성 질병으로의 적용 가능성을 보여줬다.

Keywords : 폴리페놀, 이중 에멀전, 나노전달체, 경피 약물 전달, 아토피 피부염, 알레르기
Student Number : 2021-20946